

Looking at microbial metabolism by high-resolution ^2H -NMR spectroscopy

We analyzed the applicability of high-resolution ^2H -HMR spectroscopy for the analysis of microbe metabolism in samples of mitochondrion isolated from rat liver and from aqueous extracts of homogenates of rat liver and other organs and tissues in the presence of high D_2O contents. Such analysis is possible due to the fast microbe adaptation to life in the heavy water. It is also shown that some enzymatic processes typical for the intact cells are preserved in the homogenized tissue preparations. The microbial and cellular metabolic processes can be differentiated via the strategic use of cell poisons and antibiotics.

1 **Looking at microbial metabolism by high-resolution ^2H -NMR spectroscopy**

2

3 **Victor P. Kutysenko,^{1,*} Peter M. Beskaravayny,¹ Maxim V. Molchanov,¹ Svetlana I.**

4 **Paskevich¹, Dmitry A. Prokhorov,¹ and Vladimir N. Uversky^{2,3,*}**

5

6 *¹Institute of Theoretical and Experimental Biophysics Russian Academy of Sciences, 142290*

7 *Pushchino, Russia; ²Institute for Biological Instrumentation, Russian Academy of Sciences,*

8 *142290 Pushchino, Moscow Region, Russia; Department of Molecular Medicine and USF*

9 *Health Byrd Alzheimer's Research Institute, College of Medicine, University of South*

10 *Florida, Tampa, Florida 33612, USA*

11

12 **Corresponding authors:** *To whom correspondence should be addressed: VNU, Department

13 of Molecular Medicine, University of South Florida, 12901 Bruce B. Downs Blvd., MDC07,

14 Tampa, Florida 33612, USA, Phone: 1-813-978-5816; Fax: 1-813-974-7357; E-mail:

15 vuversky@health.usf.edu; VPK, Institute of Theoretical and Experimental Biophysics of

16 Russian Academy of Science, 142290 Pushchino, Moscow region, Russia, e-mail:

17 kutysenko@rambler.ru

18 **Abstract**

19 We analyzed the applicability of high-resolution ^2H -HMR spectroscopy for the analysis of
20 microbe metabolism in samples of mitochondrion isolated from rat liver and from aqueous
21 extracts of homogenates of rat liver and other organs and tissues in the presence of high D_2O
22 contents. Such analysis is possible due to the fast microbe adaptation to life in the heavy
23 water. It is also shown that some enzymatic processes typical for the intact cells are preserved
24 in the homogenized tissue preparations. The microbial and cellular metabolic processes can
25 be differentiated via the strategic use of cell poisons and antibiotics.

26

27 **Key words:** Microbial metabolism; High resolution NMR; ^2H -HMR spectroscopy; Heavy
28 water; Microbe adaptation;

29 Introduction

30 Recent years witnessed an increased interest of researchers in the analysis of various
31 biological fluids. This research is taken now as a fundamental basis of the metabolomics,
32 which studies the metabolic profiles of animals and humans during their normal activity and
33 at various pathological conditions, as well as looks at the effects of various drugs and other
34 substances on specific organ/tissue, the whole organisms, and even on the entire ecosystem
35 (Holmes, Wilson & Nicholson, 2008; Maher *et al.*, 2008; Nicholson & Lindon, 2008).
36 Typically, term 'biological fluids' is taken as a synonym to 'body fluids' or 'biofluids' that
37 correspond to liquids originating from inside the bodies of living people, such as urine, blood,
38 saliva, sweat, cerebrospinal fluid, mucus, etc. However, this concept can be extended to
39 include water washouts and aqueous extracts of the homogenates of various organs and
40 tissues of animals (Kutyshenko *et al.*, 2007; Kutyshenko *et al.*, 2008a; Kutyshenko *et al.*,
41 2008b) and plants (Molchanov *et al.*, 2012). Addition of these somewhat artificial biological
42 fluids leads to the noticeable increase in the variability of experimental material suitable for
43 comprehensive analysis and produces substantial information related not only to the organs
44 under study, but also to the interactions of these organs with the remaining organism and with
45 specific microorganisms.

46 The close connection between plants and animals with specific microorganisms
47 constituting microbiomes or microbiotas is a well-established fact. In fact, animals, including
48 humans, constantly coexist with microorganisms, being involved in numerous symbiotic
49 interactions with various bacteria and yeast that densely populate intestines, skin, and tunica
50 mucosa of airways, pharynx and urinary tract. Furthermore, some microorganisms can get
51 access to various organs through bloodstream or other biofluids leading to the development
52 of various pathologies. The current list of human symbiotic microorganisms includes ~5,000
53 species that are uniquely distributed between 15 and 18 sites of the permanent habitat in

54 males and females, respectively (Human *et al.*, 2012a; Human *et al.*, 2012b). Since different
55 organs are biochemically different, sets of symbiotic microorganisms populating them can
56 vary between different organs within the same organism. Many members of the human
57 microbiome are conditionally pathogenic microorganisms that can provoke development of
58 various maladies if appropriate conditions are given (Tancrede, 1992; Riabichenko &
59 Bondarenko, 2007; Yu *et al.*, 2012). Under these circumstances, originally harmless and even
60 beneficiary symbiotic microorganisms can go bad and start negatively affect the normal
61 cellular and organ functions of the host organism, secreting specific toxins and ferments and
62 eventually leading to the metabolism distortion and cell death. Furthermore, by destroying the
63 host cells, microorganisms promote the release of the cell content into the extracellular
64 environment, thereby further exacerbating the course of a disease and negatively affecting the
65 overall condition of the host organism. In fact, sometimes, massive cell death can be a
66 self-propagating process, where proteins released from the dying cells affect neighboring
67 cells leading to their death and consequently generating favorable conditions for the
68 propagation of both the “own” symbiotic microorganisms of the microbiome and the
69 microorganisms introduced from the outside. Therefore, under such circumstances, therapy
70 should include both antibacterial and healing strategies.

71 In this work, the mitochondria suspension and the aqueous extracts from the homogenates
72 of several tissues are used to model cell death and organ damage (necrosis) resulting from
73 injuries and pathologies and to experimentally characterize the related processes. We propose
74 here an instrumental approach that can be used to detect and control both microbial and host
75 enzymatic processes taking place within the sites of disease origin. This approach is based on
76 the detection of the deuterium incorporation to the specific metabolism products. Here,
77 deuterium (in a form of heavy water) is added directly to the medium where the ferment
78 action and/or microorganism vital activity takes place. Our earlier analysis revealed that

79 many microorganisms can easily adapt to the conditions of high heavy water contents, and
80 presence of almost 100% heavy water does not significantly affect normal functioning of
81 certain microorganisms (Kushner, Baker & Dunstall, 1999; Molchanov *et al.*, 2012). Under
82 these conditions, deuterium can be incorporated to the substrates due to the existence of
83 efficient exchange between the protons of organic moieties of substrates and deuterium
84 present in media. Next, these deuterated substrates can be used in biochemical reactions
85 leading to the enzymatic incorporation of deuterium to the corresponding metabolism
86 products (Ewy, Ackerman & Balaban, 1988; Kushner, Baker & Dunstall, 1999; Budantsev,
87 Uversky & Kutysenko, 2010; Molchanov *et al.*, 2012). One of the most informative
88 techniques to follow the mentioned processes in biological fluids is the high-resolution NMR
89 at the deuterium nuclei, ^2H -NMR (Budantsev, Uversky & Kutysenko, 2010). In comparison
90 with proton spectra, ^2H -NMR spectra are characterized by lower resolution and lower
91 sensitivity. Furthermore, deuterium-deuterium couplings are about 40 times smaller than
92 proton-proton couplings and are therefore not observed. However, the overall shapes of
93 ^1H -NMR and ^2H -NMR spectra of organic components of are rather similar, except to the fact
94 that the multiplets seeing in ^2H -NMR spectra are presented by broader singlets due to the low
95 spin-spin interaction constants and quadrupole broadening (Emsley, Feeney & Sutcliffe,
96 1966).

97 In this work, we show the applicability of the high-resolution ^2H -NMR spectroscopy for
98 the quantitative analysis of biological fluids using preparations of mitochondria suspension
99 and aqueous extracts from rat liver homogenates as illustrative example. It is important to
100 emphasize here that the proposed approach for studying microbial and host enzymatic
101 activities based on the analysis of deuterium incorporation to the metabolic products can be
102 of wide practical use in many other cases, when high D_2O concentrations do not perturb the
103 physiological processes of the studied (Budantsev, Uversky & Kutysenko, 2010).

104

105 **Materials and Methods**

106 Mitochondria were isolated from the livers of Wistar rats using the standard protocols
107 (Belosludtsev *et al.*, 2009). Mitochondria samples used in our study were a generous gift of
108 Prof. Mironova G.D. The only modification of the isolation protocol in some preparations
109 was substitution of light water by heavy water (OOO Astrochim, Russia, 99.8%) done at our
110 request. The standard functional analysis revealed that the mitochondrion isolated using such
111 modified heavy water-based protocol were active and preserved their activity for several
112 hours after isolation. Part of mitochondrion isolated by a standard, light water-based approach
113 was subsequently treated with heavy water. The concentrations of heavy water in samples
114 were controlled using characteristic features of $^1\text{H-NMR}$ spectra.

115 Livers of the Wistar rats were a kind gift of Prof. Kichigina V.F. These animals were
116 sacrificed for the purpose of unrelated experiments (Popova, Sinelnikova & Kitchigina,
117 2008). Aqueous extracts of the rat liver homogenates were prepared using 0.40 ± 0.03 g
118 samples which were first carefully homogenized in the eppendorfs using a special sterile
119 glass spatula and then diluted with 0.75 ml heavy water (CIL, USA, 99.9%). Samples were
120 centrifuged using the microcentrifuge CM-50 (ELMI, USA) prior the NMR measurements.

121 Antibiotics gentomicin (Asparin, Germany) and amphotolecin B (Sigma) were dissolved
122 in 2 ml of D_2O to ensure final dilution of 1:200 (Solovieva *et al.*, 2008).

123 NMR spectrometer AVANCE 600 (BRUKER) with the operating frequency 600.13 MHz
124 was used in the experiments. $^1\text{H-NMR}$ spectra were measured using the spectral width of
125 8000 Hz, 90° impulse of 11 microseconds, and temperature of 298 K. As a rule, 128
126 accumulations were sufficient to obtain good signal to noise ratio. $^2\text{H-NMR}$ spectra were

127 measured using the 20W field stabilizer at the frequency of 92.12 MHz, 90°-impulse length of
128 150 microseconds, a spectrum width of 8000 Hz and 500-1000 accumulations. All the
129 measurements were made at 298 K inside the sensor.

130

131 **Results and discussion**

132 **Mitochondria from rat liver**

133 It is believed that the isolated from the rat liver mitochondria preserve their functional
134 activity *in vitro* for 1-3 hrs after isolation (Belosludtsev *et al.*, 2009). The proton NMR
135 spectrum of the suspension of mitochondria isolated using the heavy water-based protocol
136 that was collected during this initial time of the sustained mitochondrial activity is shown in
137 Figure 1A. This spectrum is dominated by the rather broad signals typical of the intracellular
138 organic molecules. Note that narrow and very intensive signals correspond in a region from
139 4.7 to 3.5 ppm to sucrose, which is present in the extracellular medium due to the
140 peculiarities of the isolation protocols (Figure 1A) (Belosludtsev *et al.*, 2009). In the
141 absorption region of the aliphatic protons (from 3.0 to 0.5 ppm), the major components are
142 broad signals corresponding to the mitochondrial membranes. After 10-12 hrs of incubation,
143 some sharp signals start to appear (see Figure 1B). These signals correspond to the organic
144 molecules extruded from the mitochondria to medium. With time, the amplitudes and number
145 of these sharp signals increase, whereas the amplitudes of broad signals proportionally
146 decrease. At this moment, spectrum contains signals of free amino acids and other organic
147 components, which are commonly detected in other biological fluids and aqueous extracts
148 from various plant and animal tissues. Figure 1C shows typical ¹H-NMR spectrum of the
149 aqueous extracts of the rat liver homogenate. Spectrum contains sharp signals of free amino
150 acids that coincide with signals detected in all major biological fluids. In fact, ¹H-NMR
151 spectra of the biological fluids studied so far are quantitatively similar possessing some

152 fluid/condition-specific qualitative differences. Comparison of Figures 1C and 1B revealed
153 that the majority of sharp signals detected in the ^1H -NMR spectrum of the aqueous extract of
154 the rat liver homogenate coincide with those in the ^1H -NMR spectrum of the mitochondria. In
155 the ^1H -NMR spectrum of the aqueous extract of the rat liver homogenate, the most
156 characteristic signals with highest intensities correspond to glucose. Proton spectra of the
157 aqueous extracts did not change neither qualitatively nor quantitatively during the
158 observation for 3-5 days.

159 Interestingly, signals in the ^2H -NMR spectrum start to appear only after incubation for
160 about 24 hrs. After another day of incubation, the ^2H -NMR spectrum is completely formed,
161 and subsequent incubation results in the increase of amplitudes of already existing signals.
162 Figure 2 represents this process by showing normalized integral intensities measured in the
163 range of 3.6-0.0 ppm of proton spectra (black circles) or in the range of 4.2-0.0 ppm of
164 ^2H -NMR spectra. The increase in the amplitudes of sharp signals in the proton spectra is
165 related to the gradual release of the intramitochondrial organic compounds resulted from the
166 destruction of mitochondrial membranes. The sharp increase in the amount of these
167 compounds is associated with the massive membrane decomposition. This process starts on
168 the second day after the mitochondrion isolation and continues for another 50 hrs, during
169 which time it slows exponentially. The increase of signals in the ^2H -NMR spectra is more
170 gradual. It is related to the activity of the mitochondrial enzymes and to the microbial
171 metabolism. On average, the integral intensities of the ^2H -NMR spectra are about 1.3-times
172 lower than amplitudes of peaks in the proton spectra.

173 During the first 27 hrs after isolation of mitochondrion, the kinetics of the formation of
174 proton- and deuterium-containing metabolites are similar due to the insignificant amounts of
175 the low molecular mass (LMM) compounds released from the destroyed mitochondria. These

176 LMM compounds serve as substrates for the metabolism of the contaminating
177 microorganisms and for the residual enzymatic activity of the mitochondrial proteins either
178 released to the medium from the destroyed mitochondria or still located inside the damaged
179 mitochondria. At longer incubation times, kinetic parameters of the observed processes
180 become more and more different. This reflects the existence of an active metabolic
181 conversion of the released substrates by microorganisms and by the residual enzymatic
182 activity of mitochondrion. Importantly, the proton spectra of mitochondrion do not
183 qualitatively change with time; i.e., no new signals appear and no old signals completely
184 disappear.

185 Figures 3A and 3B represent a pair of typical ^2H -NMR spectra measured for two
186 mitochondrial isolates randomly selected from a dozen of independent isolation performed
187 during a year using different isolation protocols (sucrose-based and mannitol-sucrose-based),
188 on the basis of D_2O and H_2O , respectively. All the recorded spectra possess close similarity to
189 each other, being mostly different in relative intensities of several peaks. Figure 3 represents
190 signal assignments based on the comparison of chemical shifts with proton spectra of known
191 metabolites from various biological fluids. These assignments took into account the presence
192 of the isotope shift and were performed using a large set of ^2H -NMR spectra of samples
193 prepared from various plant and animal sources. The major difference between spectra shown
194 in Figures 3A and 3B is in lesser amounts of ethanol and acetate in mitochondrial
195 preparations utilizing heavy water. Furthermore, in all the cases of heavy water-based
196 isolations, the rightmost signal corresponding to isotopic variant of acetate ($-\text{CD}_3$) was
197 always higher than the middle signal corresponding to $-\text{CHD}_2$, since the heavy water content
198 in these samples was $\sim 85\%$, whereas in light water-based isolations with concomitant
199 addition of D_2O , the heavy water content was at the level of 35-40%. The presence of signals

200 corresponding to ethanol, acetate and formate at 8.43 ppm (not shown) is the reflection of the
201 microbial contamination of the isolated mitochondrion.

202 Figure 3C represents a typical ^2H -spectrum of the aqueous extract of liver homogenate.
203 This spectrum, being corrected for the differences in intensity of some signals, resembles
204 spectrum of the mitochondria isolates. However, since this spectrum possesses signals
205 corresponding to ethanol, formate, and acetate, one can suggest that these samples were
206 contaminated by microorganisms. To identify signals corresponding to the products of the
207 microbial metabolism, some broad-spectrum antibiotics or sodium azide were added during
208 the sample preparation. Similar to antibiotics, sodium azide (low concentration of which are
209 used as preservative in the food industry) possess antimicrobial activities. Sodium azide
210 predominantly affects Gram-negative bacteria, suppressing their growth and development.
211 The application of both bactericides had similar outputs, and the resulting ^2H -NMR spectra of
212 the aqueous extract of liver homogenates treated with antibiotics and sodium azide were
213 identical. Figure 3D represents one of the spectra for bactericide-treated sample and shows
214 the lack of signals corresponding to ethanol, formate, and acetate, supporting their bacterial
215 origin. Therefore, resulting spectra contain only signals corresponding to the compounds
216 produced by mitochondrial enzymes under the proton-deuterium exchange conditions. The
217 liver extracts contain both substrates and ferments that participate in the enzymatic reactions
218 uncontrolled by the decomposed cells. The corresponding ^2H -NMR spectra contain alanine,
219 glycine, and lactate (Figure 3D), with alanine being the dominating component. It is known
220 that alanine accounts for ~30% of all amino acids delivered to the liver. This explains
221 relatively high concentrations of alanine in the liver preparations (see Figure 2C). In the liver,
222 alanine is converted to pyruvate, which is subsequently used for the glucose synthesis
223 (Malaisse *et al.*, 1996; Burelle *et al.*, 2000).

224 In our experiments, the samples were prepared by the mechanical homogenization of rat
225 livers. Therefore, the resulting homogenate contains some surviving cells that remain
226 functional and continue function more-or-less normally, at least for some time. Therefore,
227 these preparations can be considered as a model of severe tissue damage. Survived cells
228 continue to express proteins and possess metabolic processes supporting cell life activity.
229 Under the oxygen deficiency conditions of our experiments, the only available pathway for
230 energy generation in a cell is anaerobic glycolysis. However, the last stage of this pathway is
231 likely to be failed as evidenced by the lack of the increase in the lactate signal in the
232 corresponding $^1\text{H-NMR}$ spectra (see Figure 1C).

233 Pyruvate produced during glycolysis is converted to the alanine via the transamination
234 reaction. This reaction together with the reversed transformation of alanine to pyruvate is
235 catalyzed by the alanine transaminase also known as alanine aminotransferase (Dolle, 2000;
236 Yang *et al.*, 2009). The activity of this enzyme combined with the protein degradation and
237 membrane decomposition, together with the presence of some free alanine inside the cells
238 give likely explanation for the moderate increase in the alanine signal in the spectra of rat
239 liver homogenates during their long-term observation. The presence of deuterium in the $\text{C}\alpha$
240 position and in the methyl groups of alanine supports the enzymatic origin of alanine's
241 hydrocarbon skeleton (see Figure 4).

242 Figure 5 represents the $^2\text{H-NMR}$ spectra of mitochondria in samples containing
243 antibiotics. Comparison of spectra measured at different time points after the sample
244 preparation indicates the presence of some kinetic processes. Figure 5C shows signals
245 accumulated during the first 8 hrs of sample incubation. The most intensive signal here is a
246 signal from the glycine deuterons followed by a less intensive signal of deuterated alanine.
247 Furthermore, spectrum contains signals corresponding to the proton-deuterium exchange at

248 nitrogens of urea (5.7 ppm), glutamine (~7.6 ppm) and asparagine (~6.9 ppm). These signals
249 significantly increase after a one day incubation (see Figure 5C) but did not change much
250 during the more prolonged incubation. However, to the sixth day, spectrum undergoes further
251 changes, and signals of lactate and formic acid appear, whereas signals corresponding to the
252 nitrogen disappear. These changes reflect starting bacterial activity leading to the nitrogen
253 utilization and appearance of own metabolites. Concentrations and ratios of antibiotics were
254 carefully selected to suppress the bacterial activity and not to produce additional damage of
255 the liver cells. In these settings, the bacterial activity was sufficiently suppressed, since in the
256 absence of antibiotics, signals corresponding to lactate and ethanol were easily detectable
257 already after 2-3 days (see Figure 3).

258 The major glycine biosynthetic pathway in a cell is the one catalyzed by the serine
259 hydroxymethyltransferase, an enzyme that plays an important role in cellular one-carbon
260 pathways by catalyzing the reversible, simultaneous conversions of L-serine to glycine
261 (retro-aldol cleavage) and tetrahydrofolate to 5,10-methylenetetrahydrofolate (hydrolysis)
262 (Appaji Rao *et al.*, 2003; Scheer, Mackey & Gregory, 2005; Berdyshev *et al.*, 2011). Figure 4
263 shows that serine is synthesized in a cell from the 3-phosphoglycerate, which is one of the
264 intermediates of the glycolysis, and glutamine, which serves as the source of amine. Serine is
265 subsequently used for the protein biosynthesis and for the synthesis of phosphatidylserine that
266 constitutes typically ~15% of all membrane phospholipids. The transfer of the serine methyl
267 group to tetrahydrofolate in the presence of heavy water can be accompanied by the
268 deuteration of the CH₂-group of the newly synthesized glycine.

269 Our study revealed that high-resolution ²H-NMR spectroscopy can be successfully used
270 in metabolomics studies. Furthermore, the strategic use of antibiotics helps discriminating
271 microbial activity from enzymatic cellular processes. The major products of microbial

272 activity are organic acids, such as formate, acetate, lactate, propionate (seeing in spectra of
273 homogenates of heart muscle) and ethanol. It is important to note here that our data suggest
274 that ethanol can originate not only from the classical alcoholic fermentation but can be
275 generated via some other processes. This conclusion is based on the uneven intensities of
276 $-CD_2-$ and $-CD_3$ deuterons reproducibly detected in our experiments, whereas these signals
277 would have comparable intensities if ethanol would be exclusively generated via the
278 alcoholic fermentation pathway due to the more efficient deuteration of methylene group
279 (Kutyshenko & Iurkevich, 2000).

280 The major substrates for the ethanol formation are pyruvic acid and acetaldehyde. There
281 are several biosynthetic pathways for the production of these compounds in the organism, and
282 pyruvate and acetaldehyde can be generated from glucose (as a result of glycolysis), pentoses
283 (via pentose phosphate pathway) or from some amino acids (e.g., due to the catabolism of
284 alanine and threonine) (see Figure 4). Therefore, the ethanol formation is likely a reflection
285 of the successful development of the contaminating bacterial and fungal microbiomes. Based
286 on the characteristic patterns of the hydrogen substitution by deuterium we hypothesize that
287 the significant part of the endogenous ethanol in our settings is synthesized from the
288 deaminated amino acids (see Figure 4). For example, during the processes of alanine
289 transamination and threonine degradation, the resulting terminal CH_3 -groups of pyruvate and
290 acetaldehyde are efficiently deuterated. The subsequent fermentation of pyruvate to ethanol
291 in the presence of heavy water may be accompanied by the deuteration of ethanol's
292 $-CH_2$ -group. Resulting 2H -NMR spectra of ethanol derived from these intermediates suggest
293 almost proportional saturation of CH_3 - and $-CH_2$ -groups, in sharp contrast to the
294 disproportional saturation of these groups in ethanol molecules produced via the glucose
295 fermentation.

296

297 **Acknowledgements**

298 We are thankful to Professors Kichigina V.F., Mironova G.D. and Dr. Popova I. for
299 providing biological samples used in this study. This work was supported by a grant from
300 Russian Foundation for basic research (10-02-00996) and a program Leading Scientific
301 Schools (850.2012.4)

302 **References**

- 303 Appaji Rao, N., Ambili, M., Jala, V.R., Subramanya, H.S., Savithri, H.S. 2003.
304 Structure-function relationship in serine hydroxymethyltransferase. *Biochim Biophys*
305 *Acta* 1647: 24-29.
- 306 Belosludtsev, K.N., Saris, N.E., Belosludtseva, N.V., Trudovishnikov, A.S., Lukyanova, L.D.,
307 Mironova, G.D. 2009. Physiological aspects of the mitochondrial cyclosporin
308 A-insensitive palmitate/Ca²⁺-induced pore: tissue specificity, age profile and
309 dependence on the animal's adaptation to hypoxia. *J Bioenerg Biomembr* 41: 395-401.
- 310 Berdyshev, A.G., Gulaia, A.A., Chumak, A.A., Kindruk, N.L. 2011. [Effect of
311 N-stearoylethanolamine on free amino acid levels in rat plasma and liver with burn].
312 *Biomed Khim* 57: 446-454.
- 313 Budantsev, A.Y., Uversky, V.N., Kutysenko, V.P. 2010. Analysis of the metabolites in apical
314 area of *Allium cepa* roots by high resolution NMR spectroscopy method. *Protein Pept*
315 *Lett* 17: 86-91.
- 316 Burelle, Y., Fillipi, C., Peronnet, F., Leverve, X. 2000. Mechanisms of increased
317 gluconeogenesis from alanine in rat isolated hepatocytes after endurance training. *Am*
318 *J Physiol Endocrinol Metab* 278: E35-42.
- 319 Dolle, A. 2000. Metabolism of D- and L-[(13)C]alanine in rat liver detected by (1)H and
320 (13)C NMR spectroscopy in vivo and in vitro. *NMR Biomed* 13: 72-81.
- 321 Emsley, J.W., Feeney, J., Sutcliffe, L.H. 1966. *High resolution nuclear magnetic resonance*
322 *spectroscopy* Pergamon Press, Oxford.
- 323 Ewy, C.S., Ackerman, J.J., Balaban, R.S. 1988. Deuterium NMR cerebral imaging in situ.
324 *Magn Reson Med* 8: 35-44.
- 325 Holmes, E., Wilson, I.D., Nicholson, J.K. 2008. Metabolic phenotyping in health and disease.
326 *Cell* 134: 714-717.
- 327 Human, Microbiom, Project, Consortium 2012a. A framework for human microbiome
328 research. *Nature* 486: 215-221.
- 329 Human, Microbiom, Project, Consortium 2012b. Structure, function and diversity of the
330 healthy human microbiome. *Nature* 486: 207-214.
- 331 Kushner, D.J., Baker, A., Dunstall, T.G. 1999. Pharmacological uses and perspectives of
332 heavy water and deuterated compounds. *Can J Physiol Pharmacol* 77: 79-88.
- 333 Kutysenko, V.P., Iurkevich, D.I. 2000. [Identification of partially deuterated exometabolites
334 during culture of tea fungi in heavy water]. *Biofizika* 45: 1096-1101.
- 335 Kutysenko, V.P., Sviridova-Chailakhyan, T.A., Molochkov, N.V., Chailakhyan, L.M. 2008a.
336 A study of the organic compound composition of mouse male reproductive organs by
337 high resolution NMR. *Dokl Biochem Biophys* 420: 99-104.
- 338 Kutysenko, V.P., Sviridova-Chailakhyan, T.A., Stepanov, A.A., Chailakhyan, L.M. 2008b. A
339 study of the composition of organic substances in early mouse embryos by proton
340 magnetic resonance. *Dokl Biochem Biophys* 422: 270-273.
- 341 Kutysenko, V.P., Sviridova-Chailakhyan, T.A., Stepanov, A.A., Tsoi, N.G., Chailakhyan,
342 L.M. 2007. A study of the composition of organic compounds in mouse reproductive
343 organs at early pregnancy stages by proton magnetic resonance. *Dokl Biochem*
344 *Biophys* 414: 109-112.
- 345 Maher, A.D., Crockford, D., Toft, H., Malmodin, D., Faber, J.H., McCarthy, M.I., Barrett, A.,
346 Allen, M., Walker, M., Holmes, E., Lindon, J.C., Nicholson, J.K. 2008. Optimization
347 of human plasma 1H NMR spectroscopic data processing for high-throughput
348 metabolic phenotyping studies and detection of insulin resistance related to type 2
349 diabetes. *Anal Chem* 80: 7354-7362.

- 350 Malaisse, W.J., Zhang, T.M., Verbruggen, I., Willem, R. 1996. D-glucose generation from
351 [2-13C]pyruvate in rat hepatocytes: implications in terms of enzyme-to-enzyme
352 channelling. *Arch Biochem Biophys* 332: 341-351.
- 353 Molchanov, M.V., Kutysenko, V.P., Budantsev, A.Y., Ivanitsky, G.R. 2012. From fragments
354 to morphogenesis: NMR spectroscopy of metabolites in the apex of the roots of onion.
355 *Dokl Biochem Biophys* 442: 52-56.
- 356 Nicholson, J.K., Lindon, J.C. 2008. Systems biology: Metabonomics. *Nature* 455:
357 1054-1056.
- 358 Popova, I.Y., Sinelnikova, V.V., Kitchigina, V.F. 2008. Disturbance of the correlation between
359 hippocampal and septal EEGs during epileptogenesis. *Neurosci Lett* 442: 228-233.
- 360 Riabichenko, E.V., Bondarenko, V.M. 2007. [Role of gut bacterial autoflora and its
361 endotoxins in human pathology]. *Zh Mikrobiol Epidemiol Immunobiol*: 103-111.
- 362 Scheer, J.B., Mackey, A.D., Gregory, J.F., 3rd 2005. Activities of hepatic cytosolic and
363 mitochondrial forms of serine hydroxymethyltransferase and hepatic glycine
364 concentration are affected by vitamin B-6 intake in rats. *J Nutr* 135: 233-238.
- 365 Solovieva, M.E., Solovyev, V.V., Kudryavtsev, A.A., Trizna, Y.A., Akatov, V.S. 2008. Vitamin
366 B12b enhances the cytotoxicity of dithiothreitol. *Free Radic Biol Med* 44: 1846-1856.
- 367 Tancrede, C. 1992. Role of human microflora in health and disease. *Eur J Clin Microbiol*
368 *Infect Dis* 11: 1012-1015.
- 369 Yang, R.Z., Park, S., Reagan, W.J., Goldstein, R., Zhong, S., Lawton, M., Rajamohan, F.,
370 Qian, K., Liu, L., Gong, D.W. 2009. Alanine aminotransferase isoenzymes: molecular
371 cloning and quantitative analysis of tissue expression in rats and serum elevation in
372 liver toxicity. *Hepatology* 49: 598-607.
- 373 Yu, L.C., Wang, J.T., Wei, S.C., Ni, Y.H. 2012. Host-microbial interactions and regulation of
374 intestinal epithelial barrier function: From physiology to pathology. *World J*
375 *Gastrointest Pathophysiol* 3: 27-43.
376
377

378 **Figure legends**

379 **Figure 1.** ^1H -NMR spectra of biological fluids. **A.** mitochondrion isolated from rat liver.

380 Measurements were done immediately after mitochondrion isolation. **B.** mitochondrion

381 isolated from rat liver. Measurements were done one day after isolation. **C.** Aqueous extract

382 of the rat liver homogenate.

383

384 **Figure 2.** Time courses of changes in the integral intensities of the aliphatic part of ^1H -NMR

385 (black circles) and ^2H -NMR spectra (open circles).

386

387 **Figure 3.** ^2H -NMR spectra of biological fluids. **A.** mitochondrion isolated using D_2O -based

388 protocol. **B.** mitochondrion isolated using D_2O -based protocol. **C.** Aqueous extract of the rat

389 liver homogenate. **D.** Aqueous extract of the rat liver homogenate with sodium azide added.

390

391 **Figure 4.** Various pathways of the metabolite conversion in cytosol and mitochondrion of rat

392 liver at which hydrocarbon skeleton of resulting compounds can be deuterated.

393

394 **Figure 5.** Time course of changes in the ^2H -NMR spectra of mitochondrion samples with

395 added antibiotics. **A.** Spectrum is taken on sixth day after the sample preparation. **B.**

396 Spectrum is taken on second day after the sample preparation. **C.** Spectrum is taken 8 hours

397 after the sample preparation.

Figure 1

Figure 1

$^1\text{H-NMR}$ spectra of biological fluids. **A.** mitochondrion isolated from rat liver. Measurements were done immediately after mitochondrion isolation. **B.** mitochondrion isolated from rat liver. Measurements were done one day after isolation. **C.** Aqueous extract of the rat liver homogenate.

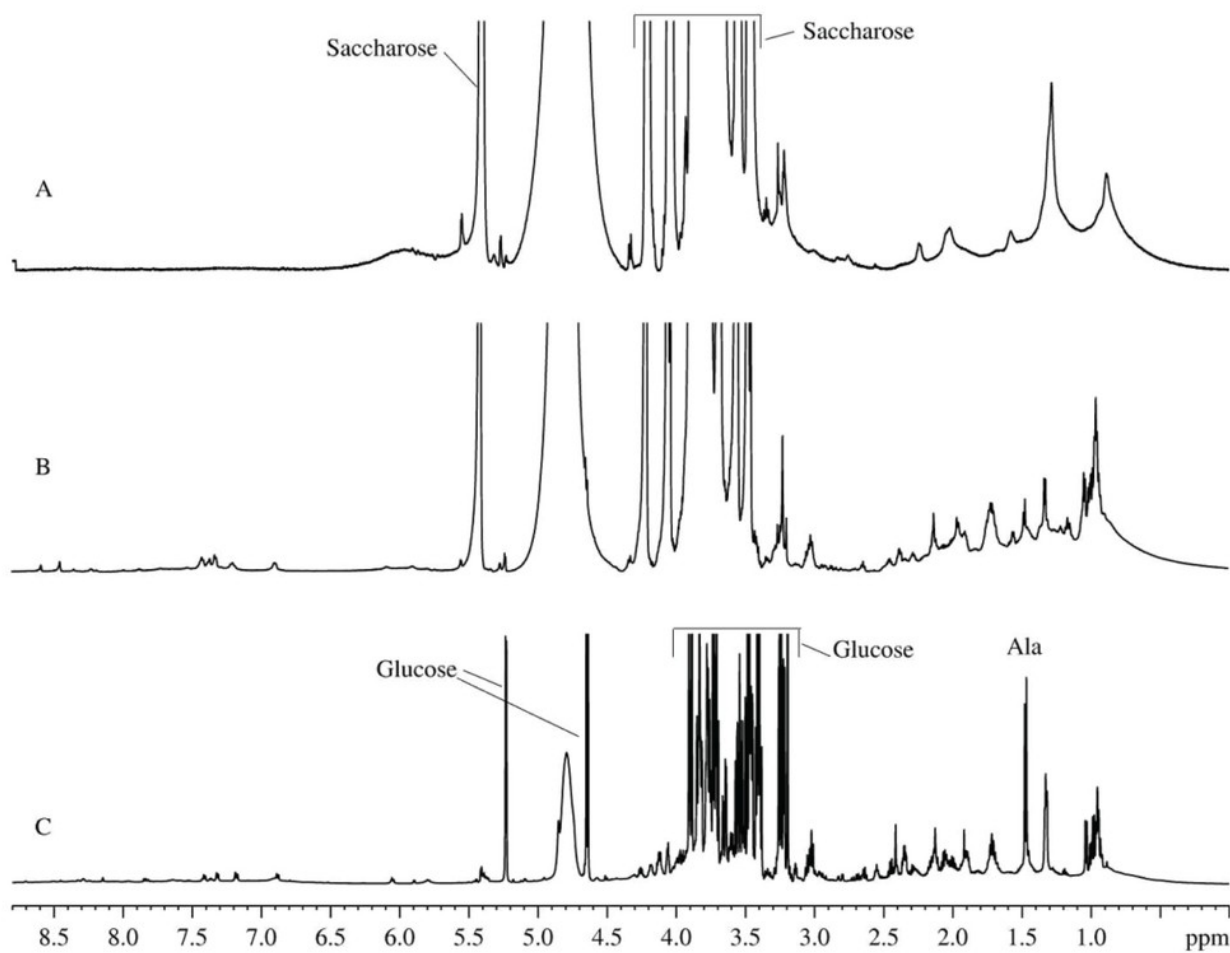


Figure 2

Figure 2

Time courses of changes in the integral intensities of the aliphatic part of $^1\text{H-NMR}$ (black circles) and $^2\text{H-NMR}$ spectra (open circles).

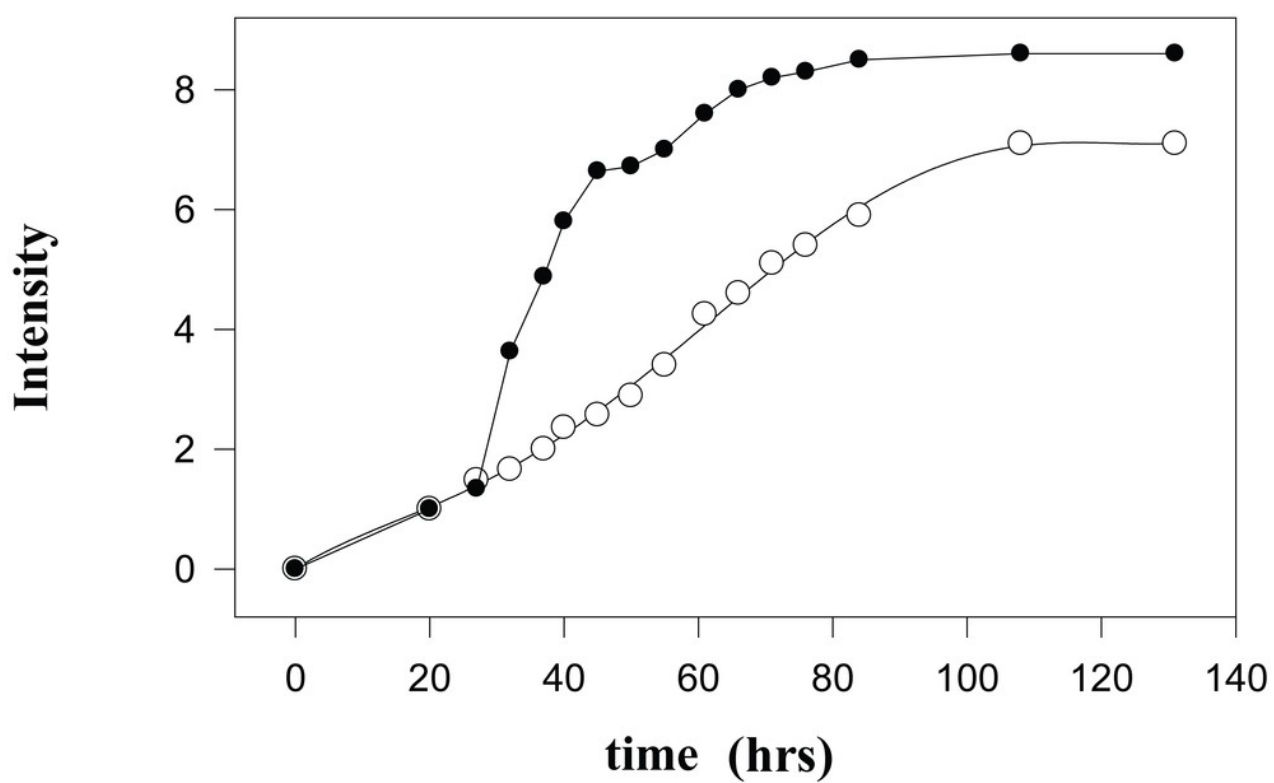


Figure 3

Figure 3

^2H -NMR spectra of biological fluids. **A.** mitochondrion isolated using D_2O -based protocol. **B.** mitochondrion isolated using D_2O -based protocol. **C.** Aqueous extract of the rat liver homogenate. **D.** Aqueous extract of the rat liver homogenate with sodium azide added.

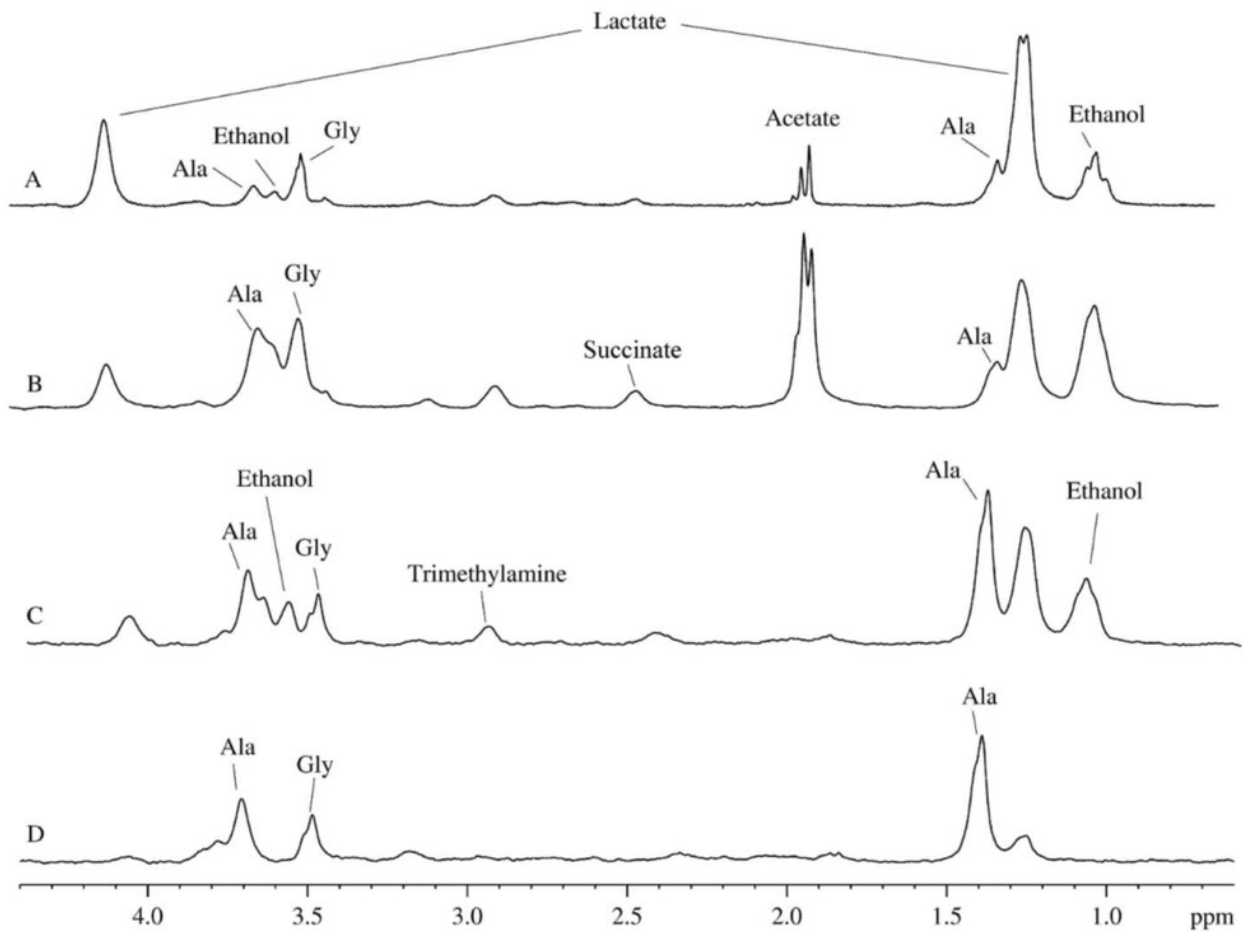
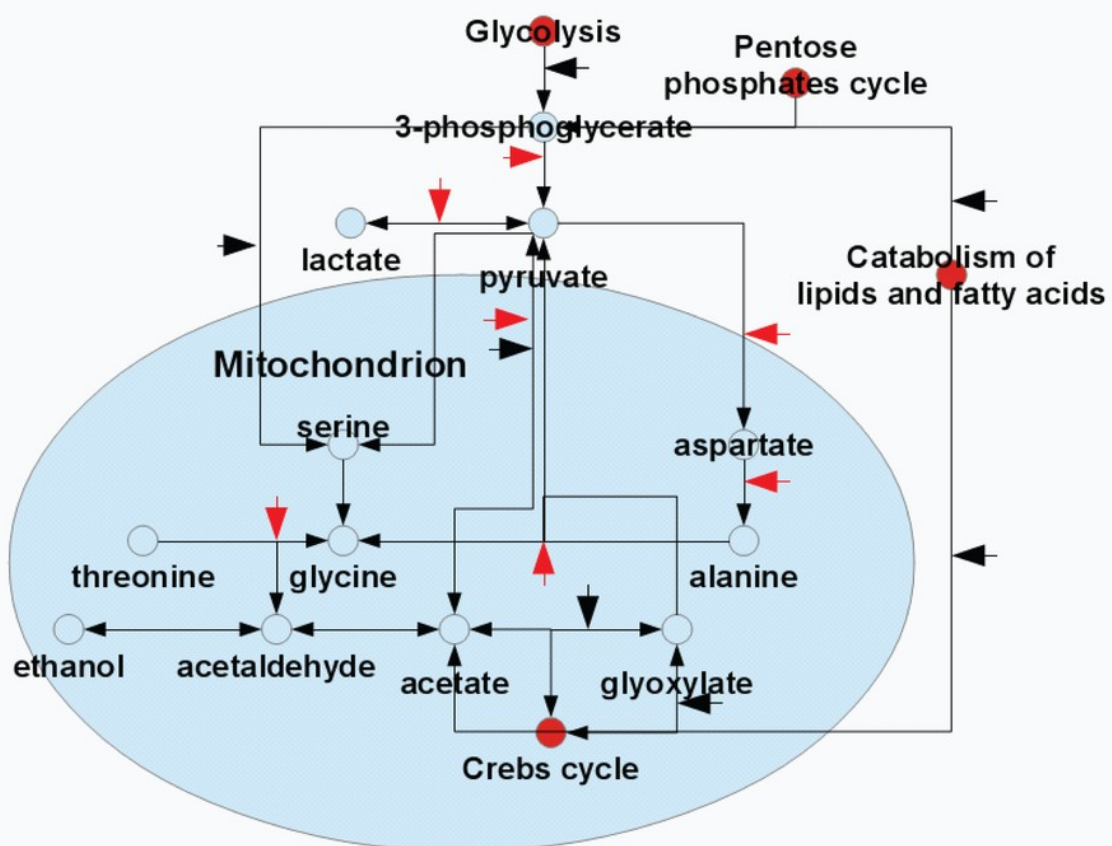


Figure 4

Figure 4

Various pathways of the metabolite conversion in cytosol and mitochondrion of rat liver at which hydrocarbon skeleton of resulting compounds can be deuterated.



- Processes where deuteration of CH₂ groups linked to the carbonyl and carboxyl groups is possible.
- Processes where deuteration of CH₂ groups linked to the amino group of amino acids and terminal CH₃ groups is possible during the cleavage of the hydrocarbon backbone.

Figure 5

Figure 5

Time course of changes in the ^2H -NMR spectra of mitochondrion samples with added antibiotics. A. Spectrum is taken on sixth day after the sample preparation. B. Spectrum is taken on second day after the sample preparation. C. Spectrum is taken 8 hours after the sample preparation.

